Polymer 49 (2008) 5636–5642

Contents lists available at ScienceDirect

Polymer

journal homepage: www.elsevier.com/locate/polymer

Synthesis of poly(methyl methacrylate)–silica nanocomposites using methacrylate-functionalized silica nanoparticles and RAFT polymerization

Pavan S. Chinthamanipeta [a], Shuji Kobukata [b], Hiromichi Nakata [c], Devon A. Shipp [a,*]

[a] Department of Chemistry and Biomolecular Science, Center for Advanced Materials Processing, Clarkson University, Potsdam, NY 13699-5810, USA
[b] Tsukuba Research Laboratories, Kuraray Co., LTD. 41, Miyukigaoka, Tsukuba, Ibaraki 305-0841, Japan
[c] Kuraray Research & Technical Center, Kuraray America Inc., 11500 Bay Area Boulevard, Pasadena, TX 77507, USA

ARTICLE INFO

Article history:
Received 29 April 2008
Received in revised form 3 October 2008
Accepted 10 October 2008
Available online 1 November 2008

Keywords:
Poly(methyl methacrylate)
Nanocomposites
RAFT polymerization

ABSTRACT

Well-defined poly(methyl methacrylate)–silica nanocomposites were produced by "grafting through" using reversible addition–fragmentation chain transfer (RAFT) polymerization. The surface of silica nanoparticle was modified covalently by attaching methacryl group to the surface using 3-methacryloxypropyldimethylchlorosilane. Polymerization of methyl methacrylate (MMA) using the 4-cyano-4-(dodecylsulfanylthiocarbonyl)sulfanyl pentanoic acid RAFT agent, produced the PMMA–SiO_2 nanocomposites. Characterization of these well-defined nanocomposites included FT-IR, gel permeation chromatography (GPC), thermogravimetric analysis (TGA), differential scanning calorimeter (DSC), transmission electron microscopy (TEM) and dynamic mechanical analysis. These results show that the T_g values are higher and the mechanical strength of the PMMA–SiO_2 nanocomposites is slightly improved when compared to bulk PMMA. Further, the molecular weight of the PMMA (up to $M_n = 100{,}000$) is controlled and the SiO_2 are well dispersed in the PMMA matrix.

1. Introduction

The spectrum of applications of a particular polymer can be broadened significantly by embedding filler nanoparticles into that polymer matrix. Such materials are called polymer nanocomposites [1,2]. The size of the nanoparticles can greatly affect the nanocomposite properties. Typically, smaller sized particles, which provide greater surface area, increase the volume fraction of the polymer matrix that interacts with the surface of the particles compared to larger particles. Thus, smaller particles can have significant effects on the properties of the nanocomposites at relatively low filler loadings (e.g. 1–5% vs. 30–50%) [3,4]. However, in order to optimize these effects, the nanoparticle should be well dispersed in the polymer matrix, which in turn is heavily dependent on the chemistry of the polymer–nanoparticle interface.

Well-dispersed polymer nanocomposites can be prepared by organically modifying the surface of the inorganic nanoparticles and then attaching polymer chains covalently to the modified surface – a process called grafting. Grafting techniques include the "grafting to", "grafting through" and "grafting from" methods. In the "grafting to" method, functional groups either at the chain end or pendant groups along the chain back bone are attached to the nanoparticle via reaction with complimentary functional groups at the nanoparticle surface [5]. This method is relatively easy, but once polymer chains populate the surface, it becomes hard for succeeding polymer chains to react with the surface of the particle, this results in relatively low grafting densities [6,7]. On the other hand, in the "grafting from" method, the surface of the particle is first modified with an initiating group followed by polymerization. In contrast with the "grafting to" method, the "grafting from" method results in high grafting densities with relatively little cross-linking [8,9]. In the "grafting through" method the surface of the particle is modified with a polymerizable group. The graft density may be relatively high compared with the "grafting to" method, but since the monomer-modified particle is multifunctional cross-linking between polymer chains may occur.

Several polymerization methods such as conventional radical [10], anionic [11,12], cationic [13–16], ring opening [17–20] and living radical polymerization (LRP) [21–27] have been used to graft polymers on various solid surfaces. Among the different methods, LRP is a versatile technique because large number of monomers can be polymerized with precise molecular weight and with narrow polydispersities. Out of the three most common LRP methods, nitroxide mediated polymerization (NMP), atom transfer radical polymerization (ATRP), reversible addition–fragmentation chain transfer (RAFT) polymerization, RAFT is arguably the most applicable technique, since most of the monomers that can be polymerized by conventional radical polymerization can be polymerized through RAFT,

* Corresponding author. Tel.: +1 315 268 2393; fax: +1 315 268 6610.
E-mail address: dshipp@clarkson.edu (D.A. Shipp).

0032-3861/$ – see front matter © 2008 Elsevier Ltd. All rights reserved.
doi:10.1016/j.polymer.2008.10.018

which is not possible with other LRP methods. The conditions for RAFT polymerization are similar to that of a conventional radical polymerization except for the addition of a RAFT agent [28–32].

Previous work has used the RAFT polymerization technique to graft polymers to silica particles either by using "grafting to" [33,34] or "grafting from" method [35–38]. Alternatively, only few papers in the literature have used the "grafting through" method [39–43] to graft polymer on the silica and none of these papers used RAFT polymerization. In this paper we report the synthesis, using the "grafting through" method (Scheme 1) and characterization of poly(methyl methacrylate) (PMMA)–silica (diameter ~20 nm) nanocomposites. To the best of our knowledge this is the first report of grafting polymer to the surface of silica by "grafting through" method using RAFT polymerization.

2. Experimental

2.1. Materials

3-Methacryloxypropyldimethylchlorosilane and acetoxyethyldimethylchlorosilane were purchased from Gelest. Tetrahydrofuran (THF) was dried over calcium hydride overnight and distilled under nitrogen. *n*-Dodecylthiol, sodium hydride, diethyl ether, iodine, sodium thiosulfate, sodium sulfate, 4,4′-azobis(4-cyanopentanoic acid), and ethyl acetate purchased from Aldrich. The synthesis of 4-cyano-4-(dodecylsulfanylthiocarbonyl)sulfanyl pentanoic acid followed the literature [32]. Methyl methacrylate (MMA) was passed through a basic alumina column to remove inhibitor and distilled under vacuum. Azobisisobutyronitrile (AIBN) purchased from Aldrich was recrystallised from methanol. Colloidal silica particles (30 wt%) with diameter of 20 nm, dispersed in methyl ethyl ketone (MEK-ST) purchased from Nissan Chemicals.

2.2. Instrumentation

NMR spectra were recorded using a Bruker Avance 400 MHz spectrometer. FT-IR spectra were recorded using a 2020 Galaxy series FT-IR instrument by the diffused reflectance (DRIFT) method. Molecular weights and molecular weight distributions or polydispersities (PD) were determined using gel permeation chromatography equipped with a Waters 515 pump, Waters auto-sampler, 2 Polymer Labs THF GPC columns, and a Viscotek LR 40 refractometer. Thermal gravimetric analysis (TGA) was performed on a Perkin Elmer Pyris1 TGA. The samples were dried at 80 °C for 12 h under vacuum and TGA was performed by heating from 30 °C to 900 °C at 10 °C/min under nitrogen atmosphere at 40 mL/min flow rate. Differential scanning calorimetry (DSC) was performed on a TA Instruments Q100. Before doing DSC, all the samples are dried under vacuum at 80 °C for 12 h. During the runs, first the samples were cooled to 25 °C and then heated to 250 °C at 10 °C/min and then cooled to 25 °C at 10 °C/min and then again heated to 250 °C at 10 °C/min. Transmission electron microscope images (TEM) were acquired using a Hitachi H-7100FA TEM instrument operating at 100 kV. Samples were sectioned at room temperature using a Reichert-Jung Ultracut S ultramicrotome. Dynamic mechanical analysis (DMA) was performed on a UBM Co., LTD. Rheogel-E-4000 DMA instrument, with temperature ranging from −150 to 200 °C at a heating rate of 3°/min, frequency of 11 Hz in tensile mode. The samples were prepared by placing 0.4 g of powder sample between Polyimide sheets, and put it between steel plates (1 mm thickness). The samples were then pressed (up to 50 kgf) and release 4 times at 200 °C to de-gas, and then pressed again with 90 kgf at 200 °C for 15 s to form the film. Specimen strips for DMA analysis were cut from the press film and measured 1.5 cm long and 0.5 cm wide. Dynamic light scattering (DLS) was performed using a Brookhaven Instruments Corp. 90Plus particle size analyzer.

2.3. Preparation of acetoxy-functionalized colloidal silica nanoparticles

Acetoxyethyldimethylchlorosilane (0.153 g), colloidal silica particles (20 mL), and 3 mL of dry THF were added to a 250 mL three necked round bottom flask and heated in a 70 °C oil bath overnight under N_2. The reaction mixture was cooled to room temperature and precipitated into hexane (400 mL). The particles were recovered by centrifugation at 3500 rpm for 20 min and dissolved in acetone (22 mL). The particles were reprecipitated in hexane (400 mL). Small quantities of acetoxy-functionalized silica particles were dried under vacuum overnight for analysis. The remaining particles were dispersed in dry THF (50 mL) under a N_2 atmosphere [36].

2.4. Preparation of methacrylate-functionalized colloidal silica nanoparticles

3-Methacryloxypropyldimethylchlorosilane (0.192 g), colloidal silica particles (24 mL), and 3 mL of dry THF were added to a 250 mL three necked round bottom flask and heated in a 70 °C oil bath overnight under N_2. The reaction mixture was cooled to room temperature and precipitated into hexane (400 mL). The particles were recovered by centrifugation at 3500 rpm for 20 min and dissolved in acetone (22 mL). The particles were reprecipitated in hexane (400 mL). Small quantities of methacrylate-functionalized silica particles were dried under vacuum overnight for analysis. The remaining particles were dispersed in dry THF (40 mL, 20 wt%) under a N_2 atmosphere [36].

2.5. Polymerization of MMA using acetoxy-functionalized silica nanoparticles

The RAFT agent 4-cyano-4-(dodecylsulfanylthiocarbonyl)sulfanyl pentanoic acid (0.0376 g), AIBN (0.0030 g), and MMA (10 mL) (molar ratios MMA:RAFT:AIBN = 1000:1:0.2), acetoxy-functionalized colloidal silica nanoparticles (5.46 mL, 7 wt% of 10 mL of MMA) and 6 mL of THF were added to a Schlenk flask and subjected to 4 freeze–pump–thaw cycles. The flask was placed under a N_2 atmosphere, and then in a 60 °C oil bath. The polymer was dissolved in THF and precipitated into methanol.

2.6. Polymerization of MMA using 4-cyano-4-(dodecylsulfanylthiocarbonyl) sulfanyl pentanoic acid RAFT agent by "grafting through"

The RAFT agent 4-cyano-4-(dodecylsulfanylthiocarbonyl)sulfanyl pentanoic acid (0.0185 g), AIBN (0.0015 g), and MMA (5 mL) (molar ratios MMA:RAFT:AIBN = 1000:1:0.2), methacrylate-functionalized silica particle suspension (2.184 mL, 7 wt% of 5 mL of MMA) and 4.7 mL of THF (total 5 mL = 0.3 mL of THF from MMA anchored silica particle suspension + 4.7 mL dry THF) were added to a schlenk flask and subjected to 4 freeze–pump–thaw cycles. The flask was placed under a N_2 atmosphere, and then in a 60 °C oil bath for 15 h. The polymer was dissolved in THF and precipitated into methanol. Three different samples with 10%, 17% and 23% silica were prepared by varying the quantities of methacrylate-functionalized silica particle suspension.

2.7. HF etching PMMA–silica nanocomposite samples

0.25 g of PMMA–silica nanocomposites were dissolved in 15 mL of toluene and 75 mg of Aliquot 336 was added. 10 mL of 5% aqueous HF was added and the mixture was stirred for 2 h. The organic layer was removed and the polymer was isolated by

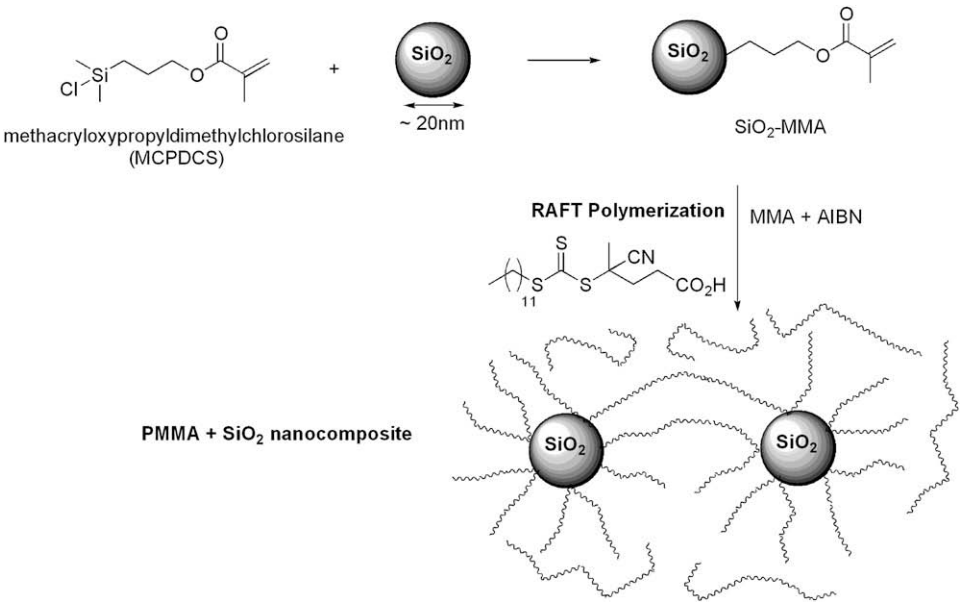

Scheme 1.

precipitation from methanol, filtered and dried under vacuum overnight.

3. Results and discussion

3.1. Preparation of methacrylate-functionalized silica nanoparticles

Methacrylate-functionalized silica nanoparticles were prepared, as shown in Scheme 1, by heating 3-methacryloxypropyldimethylchlorosilane and silica in THF. Fig. 1 shows the FT-IR of unmodified silica particles (Fig. 1a) and methacrylate-functionalized silica particles (Fig. 1b). The alkyl C–H stretching at 2968 cm^{-1} and carbonyl vibration band at 1720 cm^{-1} and peak at 1650 cm^{-1} due to C=C stretching clearly suggest the presence of methacrylate group on the silica surface. The unmodified silica shows a small peak at ~2960 cm^{-1} indicative of alkyl C–H stretches. This is likely to be due to residual solvent still present on the particle surface. The methacrylate-modified silica is similar, although the C–H stretch peak is more pronounced. Thus, the data are not conclusive that the surface was modified with the methacrylate moiety, but is consistent with the surface being methacrylated.

Fig. 2a shows the TGA curve of unmodified silica nanoparticles and Fig. 2b shows the TGA curve methacrylate-functionalized silica nanoparticles. It is evident that there is 5% weight loss. The amount of methacrylate groups on the silica particles was determined by TGA following the same calculations used by Bartholome et al. [44,45] and was determined to be 263.6 μmol/g which corresponds to 1.1 methacrylate groups/nm^2 with the assumption that density of the methacrylate-functionalized silica particles was comparable to that of bulk silica (2.07 g/cm^3) and no weight loss occurs from silica before grafting the methacrylate group.

Table 1 shows the size of the modified and non-modified nanoparticles as determined by dynamic light scatter (DLS). These data show that the mean diameter is about 25 nm for the unmodified, methacrylate-modified SiO_2 and acetoxy-modified SiO_2 (*vide infra*). Fig. 3 shows the TEM image of the methacrylate-

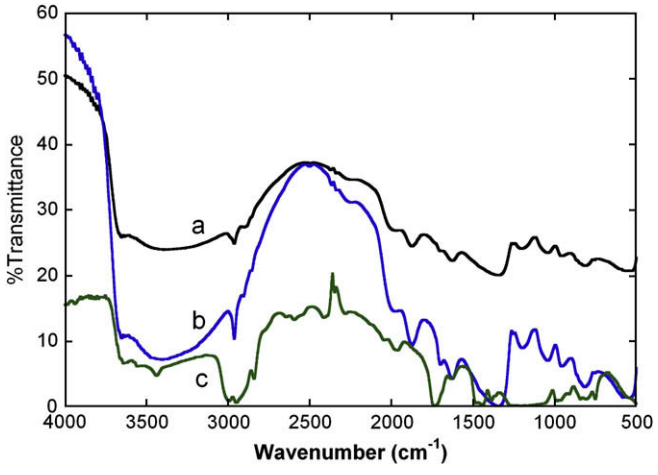

Fig. 1. FTIR of (a) unmodified silica nanoparticles, (b) methacrylate-functionalized silica nanoparticles and, (c) PMMA–silica nanocomposite with 23% silica.

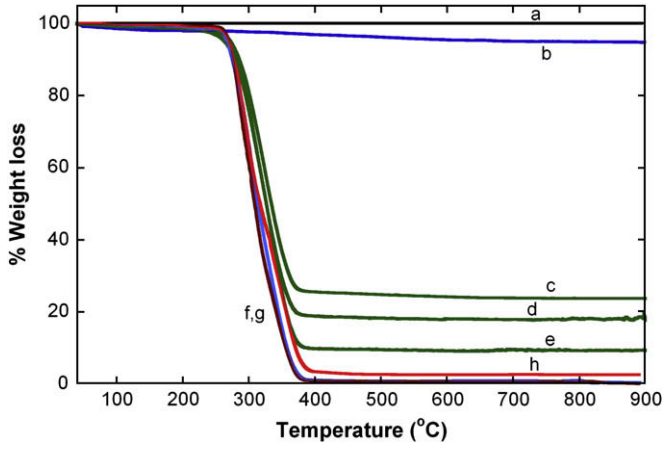

Fig. 2. TGA of (a) unmodified silica nanoparticles, (b) methacrylate-functionalized silica nanoparticles, PMMA–silica nanocomposites with (c) 23% silica (d) 17% silica (e) 10% silica, PMMA derived from nanocomposites with (f) 10% silica (g) 23% silica and, (h) 17% silica.

Table 1
DLS of non-functionalized silica particles, functionalized silica particles and PMMA silica nanocomposites.

Sample	Mean diameter (nm)
Unmodified SiO_2	26.2
Methacrylate-modified SiO_2	21.6
Acetoxy-modified SiO_2	36.6
Nanocomposite with 10% SiO_2	30.7
Nanocomposite with 17% SiO_2	38.1
Nanocomposite with 23% SiO_2	25.0

functionalized silica particles; after functionalization the particles are well dispersed and with no agglomeration.

3.2. RAFT polymerization of MMA using methacrylate-functionalized silica nanoparticles by "grafting through" and characterization of PMMA–silica nanocomposites

As mentioned above, many papers have reported the grafting of polymers onto the surface of the silica particles. However, only a few papers have reported the grafting of polymers on a silica surface using the "grafting from" method by RAFT polymerization, and furthermore no paper has reported the "grafting through" by RAFT polymerization. Li et al. [35,36] reported using 20 nm silica nanoparticles and "grafting from" using RAFT polymerization by attaching RAFT agent to the surface. Alternatively, Zhao and Perrier [37] also reported the synthesis of silica nanocomposites by "grafting from" using 35–70 μm silica particles, but used a different RAFT agent. In the latter, the RAFT agent was attached to the surface via the Z-group, whereas Li et al. used the R group of the RAFT agent. Similarly, Pan et al. reported the synthesis of silica nanocomposites by "grafting from" using 78 nm silica nanoparticles but used a different silane agent [38].

In each of these papers the syntheses of the polymer–silica nanocomposites were multi-step processes. Typically, the particle surface was modified with a silane agent and then the RAFT agent was attached to the surface via the silane agent using either the R-group or Z-group. This is then followed by RAFT polymerization. Our work reports here the synthesis of polymer nanocomposites using a simpler and more scalable process. In our approach, the particle surface is modified with a polymerizable group and dispersed in solvent. In preparing the polymer nanocomposites, the methacrylate-modified silica nanoparticles are added to RAFT polymerization. One of the benefits of this method is that the methacrylate-modified nanoparticle dispersion are quite stable, thereby reducing the possibility of aggregation which we sometimes observed when attempting the multi-step "grafting from" approach.

A secondary benefit is that by using the "grafting through" approach, the same silica content can be used to get various desired molecular weight. This is contrast to the "grafting from" method where the silica content and RAFT agent concentration are intrinsically linked. This means that samples of RAFT agent anchored silica particles with various graft densities must be synthesized to obtain the same molecular weights, or alternatively, extra untethered RAFT agent may be added. The later option, will, of course, generate untethered polymer chains.

PMMA–silica nanocomposites were synthesized by adding the methacrylate-functionalized silica nanoparticle suspension to a RAFT polymerization of MMA. Three different samples were prepared by varying the amount of the modified silica nanoparticles, keeping the ratio of monomer, RAFT agent and AIBN constant. The molecular weight of the cleaved PMMA was measured by GPC. Table 2 shows the molecular weight of polymer of three samples after etching the silica with HF. In each case, the M_n was relatively high (75,000–100,000) and the M_w/M_n around 1.25–1.35. These are typical values for RAFT polymerization of MMA.

Table 2
% Silica content, molecular weight and polydispersity of PMMA after HF etching.

% silica	M_n (after etching)	M_w/M_n
10%	103,700	1.25
17%	78,800	1.33
23%	85,200	1.25

Fig. 1 shows the FT-IR spectra for the unmodified silica, the methacrylate-modified silica and the PMMA–silica nanocomposites (Fig. 1c). Fig. 1c has a broad peak at 2900 cm^{-1} resulting from large amounts of alkyl groups from PMMA, along with a peak at 1720 cm^{-1} indicating carbonyl stretching. Thus, the IR data show clear evidence of polymer in the nanocomposite samples.

Fig. 2 shows the TGA curves of unmodified and modified silica, and the PMMA–silica nanocomposites. They clearly show the three different samples of nanocomposites with 10%, 17% and 23% silica

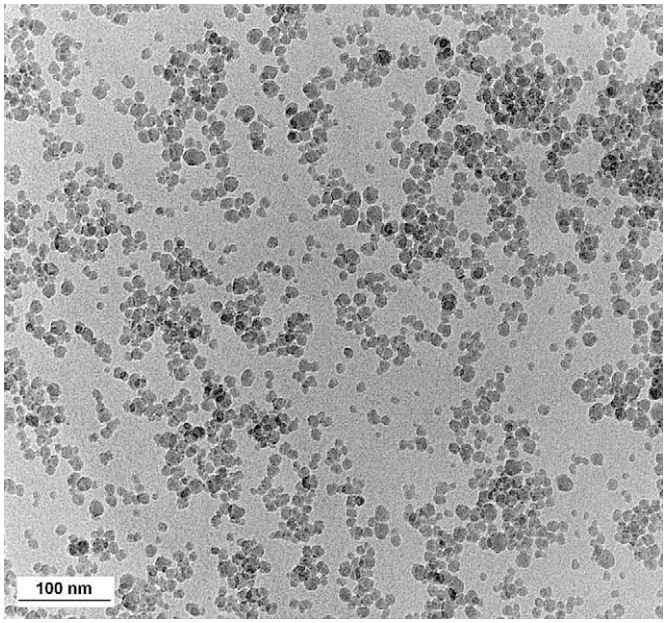

Fig. 3. TEM images of methacrylate-functionalized SiO_2 particles.

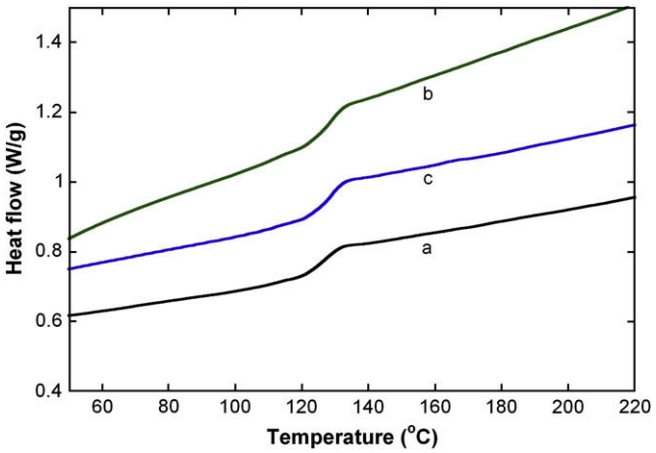

Fig. 4. DSC traces of PMMA–silica nanocomposites with (a) 10% silica (b) 17% silica and, (c) 23% silica.

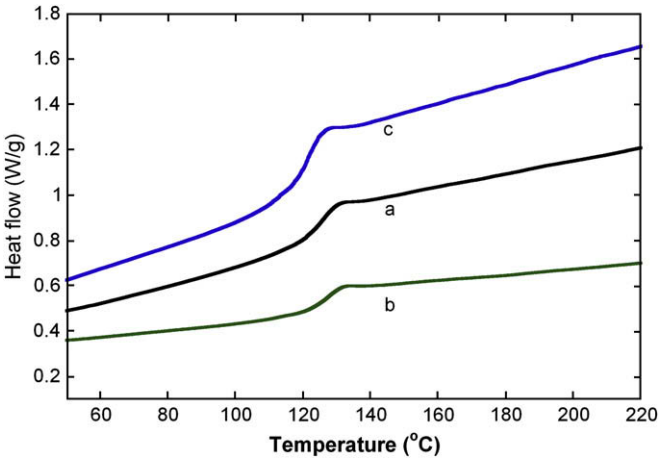

Fig. 5. DSC traces of PMMA obtained from nanocomposites with (a) 10% silica (b) 17% silica and, (c) 23% silica (after HF etching).

loadings. The TGA data indicate that there is no weight loss up to 280 °C for the PMMA nanocomposites and completely decomposes around 370 °C. Fig. 2a shows the TGA curve of unmodified silica nanoparticles and Fig. 2b shows the TGA curve methacrylate-functionalized silica nanoparticles. Fig. 2c–e is the TGA curves of PMMA–silica nanocomposites with different silica loadings, Fig. 2f–h is the TGA curves of PMMA after removal of the silica with HF. Fig. 2f and g shows the PMMA derived from nanocomposite with 10% silica and 23% silica, respectively, and indicate no silica present in these samples after etching. The curve shown in Fig. 2h represents the PMMA derived from the nanocomposite with 17% silica and shows a small amount of silica present, presumably due to incomplete etching with HF.

Depending on the molecular weight, the typical T_g of the pristine PMMA varies from 95 °C to 110 °C. Fig. 4a shows the second heating profile of the 10% silica sample, Fig. 4b shows the 17% silica sample and Fig. 4c shows the 23% silica sample. The T_g values are around 125 °C for each of these samples. Fig. 5 shows the DSC curves of PMMA samples after the silica has been removed by HF etching. In these samples, the T_g values were around 120 °C. Thus, after the removal of silica all the samples show slightly decreased T_g values, although these are still slightly higher than the standard literature value.

The PMMA nanocomposites all formed transparent films. Fig. 6 shows the TEM images of samples at low magnification, the silica nanoparticles are well dispersed without aggregation. The TEM images in Fig. 7 are at high magnification and show the sizes of the particles range between 15 and 30 nm, again without any

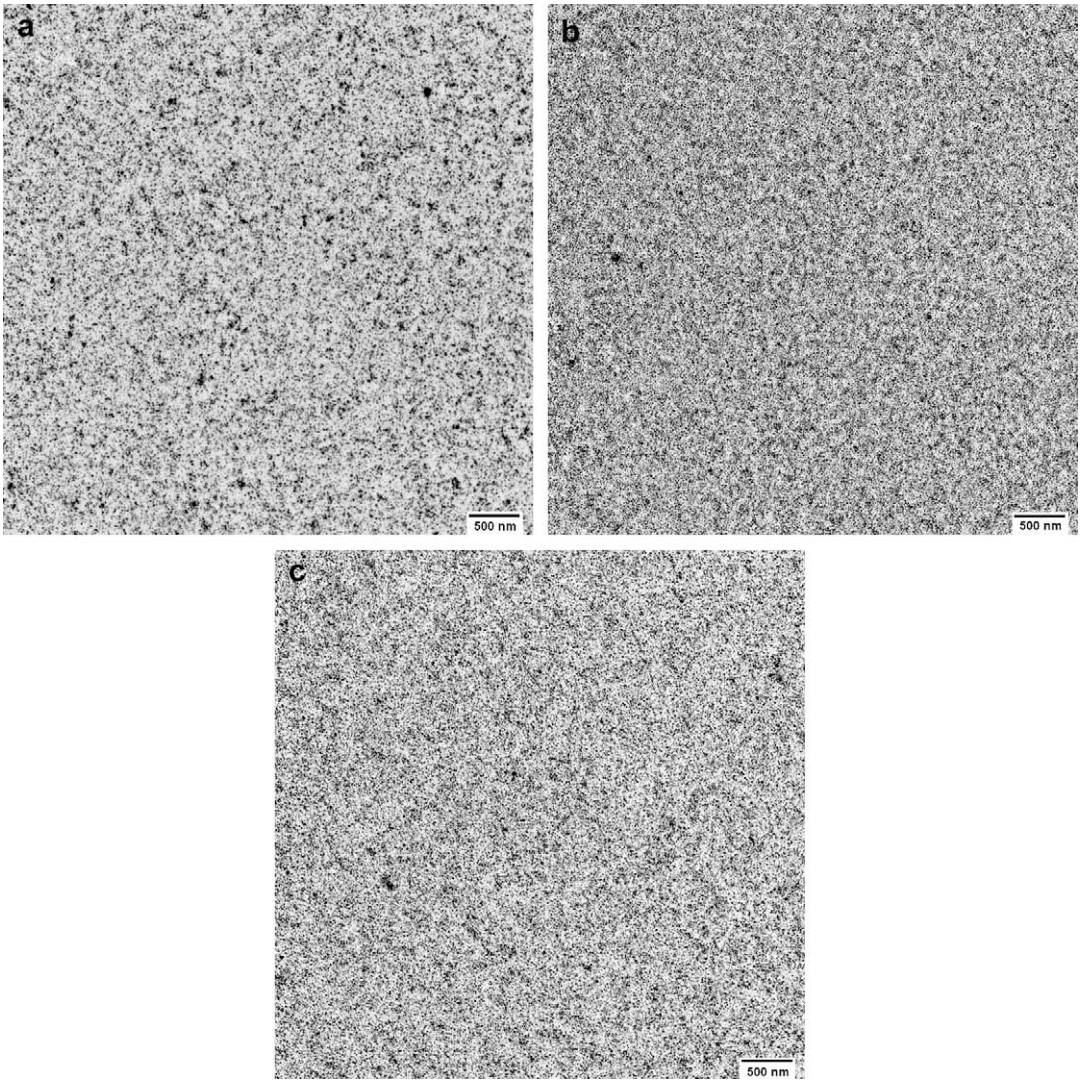

Fig. 6. TEM images of PMMA–silica nanocomposites (low magnification). (a) 10% silica (b) 17% silica and, (c) 23% silica.

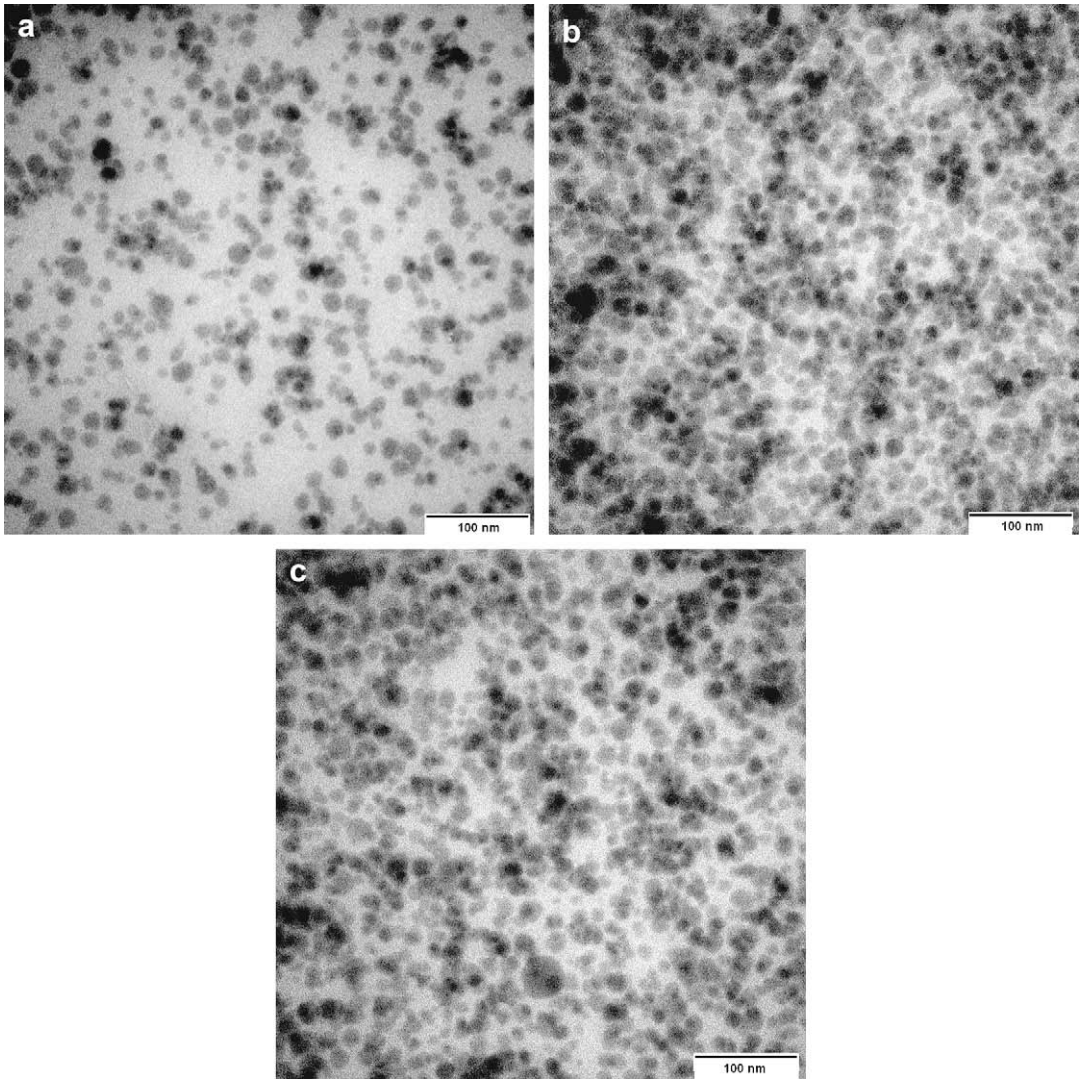

Fig. 7. TEM images of PMMA–silica nanocomposites (high magnification). (a) 10% Silica (b) 17% silica and, (c) 23% silica.

aggregation. The DLS data in Table 1 also show the particles size of the PMMA nanocomposites is in between 25 and 40 nm which supports the conclusions from TEM that the silica are well dispersed in the PMMA matrix.

The dynamic viscoelasticity of the nanocomposite materials was also measured, as shown in Fig. 8. These data indicate that the inclusion of the silica generally lead to a small increase in both the storage and loss modulus, and an increase in the temperature for the tan δ peak. These results are in general agreement with the DSC results reported above. Hence, in addition to improved thermal properties, these PMMA–silica nanocomposites exhibit enhanced mechanical properties.

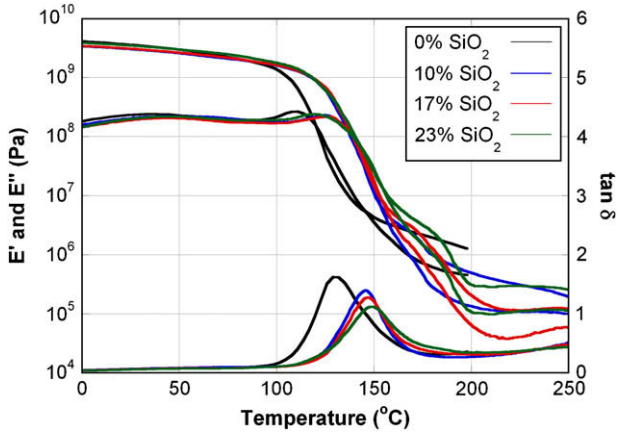

Fig. 8. Dynamic viscoelasticity of PMMA and PMMA–silica nanocomposites.

3.3. Comparison between non-polymerizable and polymerizable SiO_2 surface modification

It is of interest to compare the effect of having a polymerizable group present on the surface of the SiO_2 nanoparticles on dispersability and incorporation into the PMMA matrix. To this end, the surface of the silica particle was modified with non-polymerizable group, acetoxyethyldimethyl silane, which should mimic the methacrylate group previously used. These acetoxy-modified nanoparticles were prepared in a similar way to the methacrylated nanoparticles, and used in RAFT polymerizations of MMA. GPC analysis of the polymer showed an M_n of 72,000 and PD of 1.29. Furthermore, we found that upon precipitation of the resulting PMMA into methanol, no silica was present (as determined by TGA). Repeating the reaction but removing unreacted MMA *in vacuo* gave similar GPC analysis but the TGA showed a 7 wt% SiO_2 loading. Based on these results, we conclude that the

acetoxy-modified nanoparticles are not covalently bound to the polymer and after precipitation the particles are remaining in the methanol and are not being filtered off with the polymer.

4. Conclusions

A convenient procedure was reported in which the surface of the silica particles was successfully functionalized with methacrylate functional group using 3-methacryloxy-propyldimethylchlorosilane agent. PMMA was successfully grafted onto the silica particles by "grafting through" using the methacrylate-functionalized silica particles in a RAFT polymerization. The PMMA–silica nanocomposite T_g values are slightly higher than neat PMMA. TEM shows the silica particles are well dispersed and dynamic viscoelastic data show these PMMA–silica nanocomposites exhibit better mechanical properties in addition to improved thermal properties.

Acknowledgements

We thank Kuraray America Inc., the Center for Advanced Materials Processing (CAMP) at Clarkson University (a New York State Center for Advanced Technology), and the Department of Chemistry and Biomolecular Science for financial support.

References

[1] Yang F, Nelson GL. J Appl Polym Sci 2004;91:3844–50.
[2] Kashiwagi T, Morgan AB, Antonucci JM, Vanlandingham Jr MR, RHH, Awad WH, et al. J Appl Polym Sci 2003;89:2072–8.
[3] Ash BJ, Siegel RW, Schadler LS. Macromolecules 2004;37:1358–69.
[4] Ash BJ, Rogers DF, Wiegand CJ, Schadler LS, Siegel RW, Benicewicz BC, et al. Polym Compos 2002:23.
[5] Yoshikawa S, Tsubokawa N. Polym J 1996;28:317–22.
[6] Mansky P, Liu Y, Huang E, Russell TP, Hawker C. Science 1997:275.
[7] Lyatskaya Y, Balazs AC. Macromolecules 1998;31:6676–80.
[8] Edmondson S, Osborne VL, Huck WTS. Chem Soc Rev 2004:33.
[9] Radhakrishnan B, Ranjan R, Brittain WJ. J Soft Matter 2006;2:386–96.
[10] Sugimoto H, Daimatsu K, Nakanishi E, Ogasawara Y, Yasumura T, Inomata K. Polymer 2006;47:3754–9.
[11] Jordan R, Ulman A. J Am Chem Soc 1999;121:1016–22.
[12] Zhou Q, Wang S, Fan X, Advincula R. Langmuir 2002;18:3324–31.
[13] Zhao B, Brittain WJ, Zhou W, Cheng SZD. J Am Chem Soc 2000;122:2407–8.
[14] Jordan R, Ulman A. J Am Chem Soc 1998;120:243–7.
[15] Vidal A, Guyot A, Kennedy JP. Polym Bull 1982:401–7.
[16] Vidal A, Guyot A, Kennedy JP. Polym Bull 1980;2:315–27.
[17] Juang A, Scherman OA, Grubbs RH, Lewis NS. Langmuir 2001;17:1321–3.
[18] Joubert M, Delaite C, Bourgeat-Lami E, Dumas P. Macromol Rapid Commun 2005;26:602–7.
[19] Yang Y, Wu D, Li C, Liu L, Cheng X, Zhao H. Polymer 2006;47:7374–81.
[20] Joubert M, Delaite C, Bourgeat-Lami E, Dumas P. J Polym Sci Part A Polym Chem 2004;42:1976–84.
[21] Werne TV, Patten TE. J Am Chem Soc 1999;121:7409–10.
[22] Matyjaszewski K, Miller PJ, Shukla N, Immaraporn B, Gelman A, Luokala BB, et al. Macromolecules 1999;32:8716–24.
[23] Werne TV, Patten TE. J Am Chem Soc 2001;123:7497–505.
[24] Ohno K, Koh K-M, Tsujii Y, Fukuda T. Macromolecules 2002;35:8989–93.
[25] Carrot G, Diamanti S, Manuszak M, Charleux B, Vairon J-P. J Polym Sci Part A Polym Chem 2001;39:4294–301.
[26] Pyun J, Jia S, Kowalewski T, Patterson GD, Matyjaszewski K. Macromolecules 2003;36:5094–104.
[27] Jeyaprakash JD, Samuel S, Dhamodharan R, Rühe J. Macromol Rapid Commun 2002:277–81.
[28] Shipp DA. J Macromol Sci Part C Polym Rev 2005;45:171–94.
[29] Chiefari J, Chong YKB, Ercole F, Krstina J, Jeffery J, Le TPT, et al. Macromolecules 1998;31:5559–62.
[30] Schilli C, Lanzendorfer M, Muller AHE. Macromolecules 2002;35:6819–27.
[31] Moad G, Rizzardo E, Thang SH. Aust J Chem 2005;58:379–410.
[32] Moad G, Chong YK, Postma A, Rizzardo E, Thang SH. Polymer 2005;46:8458–68.
[33] Bridgera K, Fairhurstb D, Vincen B. J Colloid Interface Sci 1979;68:190–5.
[34] Vincent B. Chem Eng Sci 1993;48:429–36.
[35] Li C, Benicewicz BC. Macromolecules 2005;38:5929–36.
[36] Li C, Han J, Ryu CY, Benicewicz BC. Macromolecules 2006;39:3175–83.
[37] Zhao Y, Perrier S. Macromolecules 2006;39:8603–8.
[38] Liu C-H, Pan C-Y. Polymer 2007;48:3679–85.
[39] Espiard P, Guyot A. Polymer 1995;36:4391–5.
[40] Sunkara HB, Jethmalani JM, Ford WT. Chem Mater 1994;6:362–4.
[41] Asher SA, Holtz J, Liu L, Wu Z. J Am Chem Soc 1994;116:4997–8.
[42] Bourgeat-Lami E, Lang J. Colloid Interface Sci 1998;197:293–308.
[43] Barthet C, Hickey AJ, Cairns DB, Armes SP. Adv Mater 1999;11:408–10.
[44] Bartholome CL, Beyoua E, Bourgeat-Lamib E, Chaumonta P, Zydowicz N. Polymer 2005;46:8502–10.
[45] Bartholome C, Beyou E, Bourgeat-Lami E, Chaumont P, Lefebvre F, Zydowicz N. Macromolecules 2005;38:1099–106.